

F-16 FLIGHT TEST RESULTS OF A MEMS IMU CALIBRATION AND ALIGNMENT ALGORITHM

Kevin J. Shortelle and William R. Graham
System Dynamics International, Inc.
5346 SW 91st Terrace
Gainesville, FL 32608

ABSTRACT

This paper presents the results of an effort to develop and flight test an innovative transfer alignment algorithm designed to align and calibrate a low-performance MEMS IMU installed in an air-launched munition. The algorithm, referred to as MEMS IMU Calibration and Alignment (MICA), employs a 19-state Kalman filter designed to align the IMU and calibrate the IMU's low-grade gyros relative to an aircraft-grade INS. The algorithm augments conventional integrated-velocity-match (IVM) measurements with a yaw attitude-match measurement. The yaw attitude-match measurement continually calibrates the MEMS z-gyro drift and bounds IMU heading error growth during straight-and-level segments of the aircraft's alignment trajectory. Laboratory and van tests were conducted to evaluate the performance of the MICA algorithm in a low to moderate dynamic environment. Following van tests, the equipment was installed on an F-16 and captive-carry flight tests were conducted. Flight tests involved standard, multi-minute alignment trajectories followed by post-alignment trajectories specified to represent the dynamics of a released weapon. For each test, the IMU was transfer aligned with both the MICA filter and the conventional IVM filter using two separate software channels to maintain two independent alignment and navigation solutions. Initial flight test results indicate that the MICA filter improves IMU alignment and calibration accuracy relative to the IVM filter, resulting in unaided navigation performance similar to that expected for a 5 – 10 deg/hr system.

1. INTRODUCTION

The U.S. Air Force is currently pursuing several technology programs which specify a need for small, low-cost IMUs for tactical air-launched weapons. Specifically, investigations are underway to determine the suitability of micro-electromechanical sensors (MEMS) and ultimately MEMS-based IMUs for these applications. In the near future, MEMS IMUs are expected to be produced which exhibit close to 1 mg accelerometer errors (using conventional accelerometers) and 50-100 deg/hr gyro errors (using MEMS gyros). Although the accelerometer errors are

acceptable for tactical-grade systems, the gyro errors are not. In fact, MEMS gyro errors are approximately one to two orders-of-magnitude larger than those currently associated with the more mature but more costly optical gyro IMUs (i.e., RLGs and FOGs). For most tactical weapon-system applications, the MEMS gyro errors alone would induce a prohibitively large weapon CEP (e.g., hundreds of meters), virtually eliminating MEMS IMUs from serious consideration. However, if the MEMS gyros can be substantially calibrated during pre-launch alignment, and if the calibration can be maintained during weapon flight, MEMS IMUs may still be viable candidates for tactical systems.

In this paper, a novel transfer alignment algorithm is presented which is capable of calibrating the low-performance MEMS gyros and accurately aligning the MEMS IMU during a typical pre-launch alignment sequence. This algorithm, referred to as the MEMS IMU Calibration and Alignment (MICA) algorithm, is a straightforward modification of a conventional transfer alignment algorithm. In the conventional algorithm, a Kalman filter processes either integrated-velocity-match measurements (currently used by JDAM and earmarked for WCMD) or velocity-match measurements while the aircraft executes a prescribed alignment trajectory. The MICA algorithm augments the conventional procedure by processing an additional attitude-match measurement. Simulation results indicate that a MEMS IMU aligned with the MICA algorithm can achieve tactical navigation accuracy over the relatively short-duration (<100 sec) weapon trajectories of interest. Consequently, using the MICA algorithm, tactical weapon systems can potentially reap the benefits of a small, low-cost MEMS IMU without sacrificing system accuracy.

This remainder of this paper is organized as follows. Section 2 summarizes the MICA equipment suite, the MICA filter and accompanying transfer alignment measurement equations, and simulation results. Section 3 summarizes laboratory test results while Section 4 summarizes van test results. Flight test results are then presented in Section 5. Overall conclusions are presented in Section 6.

2. MICA EQUIPMENT AND FILTER DESIGN

2.1 MICA EQUIPMENT

The MICA equipment suite includes a brassboard MEMS IMU and off-the-shelf conventional hardware selected to be consistent with modern air-to-surface weapon systems. Specifically, the MICA equipment suite consists of a:

- Honeywell brassboard MEMS IMU
- Honeywell H-423 RLG strapdown INS
- Honeywell Integrated Flight Management Unit (IFMU) with embedded IEC GPS receiver card.
- Advantech AMD-K6-2/300 MHz computer
- Termiflex controller.

The brassboard IMU is a “hybrid” device developed by Honeywell which incorporates Draper TFG-14 MEMS gyros (100 deg/hr fixed drift) and conventional RBA-500 accelerometers (< 1mg fixed bias) packaged within a HG-1700 case. The TFG-14 gyros are based on the Coriolis-force tuning fork principle. Here, two vibrating proof masses suspended by flexural supports are driven in opposite directions by electrostatic motors to maintain in-plane oscillation. When an angular rate is applied about the input axis, which is parallel to the proof mass plane and normal to the vibration vector, one of the vibrating masses will lift up out of the plane while the other moves down. The resulting up/down motion, proportional to the angular rate, is measured by capacitive sense plants beneath the proof masses.

During laboratory tests conducted by Honeywell and System Dynamics, the TFG-14 gyros exhibited an accuracy consistent with a fixed drift rate of 100 deg/hr (one sigma), an in-run stability drift rate of 10 deg/hr (one sigma) with a correlation time of 300 sec, a scale factor error of 500 ppm (one sigma), and an angle random walk of 0.1 deg/root-hr. A detailed error characterization can be found in Ref. 5.

The H-423 INS is an aircraft-quality (0.8 nmi/hr) strapdown navigation system designed to conform to the USAF Standard INS specification (SNU 84-1). It incorporates GG1342 RLGs (0.004 deg/hr drift) and QA-2000 accelerometers. The INS is the reference to which the MEMS IMU is aligned and calibrated. The IFMU incorporates a conventional HG-1700 IMU which includes GG-1308 RLGs (1 deg/hr drift) and RBA-500 accelerometers. Note that the IFMU is not involved in the MICA transfer alignment algorithm. Rather, it is used to provide inertial truth data (i.e., ΔV s and $\Delta\theta$ s) which are compared with similar data provided by the MEMS IMU during post-test analyses.

The MICA computer is a ruggedized AMD-K6-2/300 MHz PC which hosts the MICA Kalman filter transfer alignment algorithm and the MEMS IMU strapdown navigation equations. The computer is equipped with a MIL-STD-1553B interface card for communication with the H-423 INS, and three RS-422 interface cards which provide asynchronous serial communication with the IMU, IFMU, and Termiflex controller. In the laboratory configuration, the computer is interfaced with a desktop monitor, keyboard, and mouse. However, in the flight configuration, these peripherals are replaced by the Termiflex controller. The Termiflex controller is a small control display unit used to control and monitor MICA flight tests from the cockpit.

During flight tests, the H-423 INS was installed in the ammo drum located directly behind the cockpit. The Termiflex controller was mounted in the cockpit within easy reach of the pilot. All other MICA equipment was installed in a general instrumentation (GI) pod attached to weapon station #3 of the F-16. The MICA equipment interfaces and F-16 locations are illustrated in Figure 2.1-1

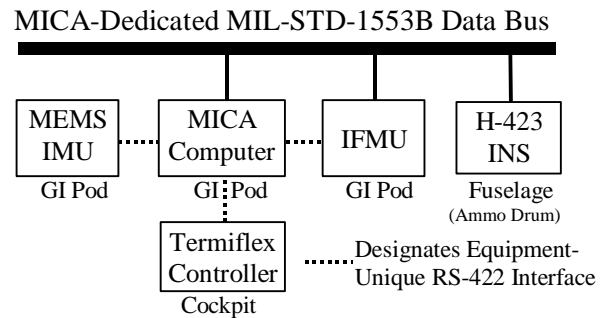


Figure 2.1-1 MICA Flight Configuration Interface

2.2 MICA FILTER DESIGN

The MICA Kalman filter was designed by first developing a full-order optimal transfer alignment Kalman filter and then downsizing the optimal filter to achieve a practical reduced-order design. The optimal filter incorporates a high-fidelity truth model which precisely models (in state-space form) all significant linear error sources associated with the transfer alignment equipment and procedure. While not practical for real-time implementation (due to its large state size and sensitivity), the optimal filter is typically employed to provide the performance benchmark for the subsequent reduced-order filter design.

Filter States and Models: The MICA optimal filter was formulated to faithfully characterize the error behavior of the MEMS brassboard IMU and H-423 INS during transfer alignment. Specifically, the optimal filter included 86 states to characterize MEMS IMU navigation errors, IMU accelerometer and gyro errors, IMU time-tag errors, INS navigation errors, and wing deformation.^{1,2} A filter sizing study conducted using System Dynamics’ (real-world/filter-

world) transfer alignment covariance simulation, TRANSIM, determined that 67 of these states could either be eliminated from the design or combined with other states without significantly degrading alignment accuracy. The remaining 19 states comprised the MICA filter design. The MICA filter state vector is summarized in Table 2.2-1.

Table 2.2-1 MICA Filter Design

STATE	DESCRIPTION	INITIAL 1σ VALUE	UNITS
1-3	Integrated Velocity Errors	1000	m
4-6	IMU Velocity Errors	10	m/sec
7-9	IMU Attitude Errors	.04,.04,.01	rad
10-12	IMU Accelerometer Biases	0.4	mg
13-15	IMU Gyro Fixed Drifts	100,100,20	deg/hr
16,17	IMU Time-Tag Errors	0.002, 0.01	sec
18	Yaw Rigid Misalignment	0.01	rad
19	Yaw Flexure	0.001	rad

Table 2.2-1 also presents the one-sigma values used to initialize the filter's estimation-error covariance matrix (P) diagonal elements. The one-sigma values for the first nine states were selected to be relatively large in order to force the filter to heavily weight the first set of measurements, thereby re-initializing the IMU's strapdown equations. This procedure ameliorates potential time delays incurred during the initialization process.

The one-sigma values for the inertial sensor error states were selected to characterize the expected error behavior of the sensors while providing a robust filter design. For instance, the accelerometer errors were modeled using 0.4 mg values, rather than the specified 0.8 mg values, in order to discourage the filter from estimating marginally observable accelerometer errors. Furthermore, while the x and y (i.e., roll and pitch) gyro errors were modeled with the specified 100 deg/hr one-sigma values, the z (yaw) drift was modeled with a much smaller 20 deg/hr value. The 20 deg/hr value was selected primarily as a tradeoff to avoid accuracy problems with the IVM-only filter during periods of lengthy straight-and-level flight (due to z-gyro drift unobservability).

The inertial sensor errors were modeled as random walk processes in an effort to characterize both the fixed bias and in-run stability behavior of each error with a single state. The fixed bias portion was characterized by the corresponding one-sigma value initialized in the P matrix while the in-run stability portion was characterized by the corresponding one-sigma value stored in the process-noise covariance matrix, Q_d . Although not shown in Table 2.2-1, gyro angle random walk errors (0.1 deg/root-hr) were also included in the filter design. These errors were modeled as white noise processes driving the IMU's attitude error states (i.e., as diagonal elements in the Q_d matrix corresponding to the attitude error states).

The IMU time-tag and yaw flexure errors were modeled as first-order markov processes to capture the time-varying

(correlated) behavior of these errors. Yaw flexure is a particularly important error source for attitude-match filters since low-frequency relative motion between the INS and IMU during alignment about the yaw axis inhibits observability of yaw gyro drift. Fortunately, based on test data, yaw flexure is expected to be relatively small, as evidenced by its modeled 1 mrad one-sigma value. (Further modeling details are provided in Ref 5.)

Filter Measurements: The MICA filter was designed to process three (x, y, and z) integrated-velocity-match (IVM) measurements and a yaw attitude-match (AM) measurement at each measurement update time. (Although initially considered, the roll and pitch AM measurements were discarded from the final filter design based on simulation results which deemed them to be unnecessary.) The nominal measurement update rate was 0.5 Hz, although slower rates (e.g., 1/6 Hz) were simulated and found to be acceptable. Immediately following each update, the filter's state estimates were fed back to the strapdown navigation algorithm to correct the computed IMU navigation solution and calibrate the IMU's inertial sensors.

The IVM measurements were formed by differencing the change-in-position indicated by the aircraft INS (since the start of alignment) with that indicated by the IMU over the same time frame. The yaw AM measurement was formed by first pre-multiplying the body-frame to local-level frame transformation matrix indicated by the INS with the transpose of the same matrix indicated by the IMU, and then averaging the corresponding (skew-symmetric) off-diagonal element to form the yaw measurement¹.

Simulation Results: Simulation results generated by TRANSIM indicated that the MICA filter is expected to:

- (1) Achieve an alignment accuracy close to 1 mrad (one sigma) in all three axes
- (2) Calibrate the MEMS gyros from 100 deg/hr to better than 5 deg/hr, regardless of the alignment maneuvers executed by the aircraft
- (3) Inhibit heading error growth during straight-and-level segments following the completion of an alignment maneuver.

The second and third results are a direct consequence of the yaw AM measurement. Specifically, the yaw AM measurement affords continuous observability of IMU z-gyro drift, thereby bounding the growth rate of IMU heading error during low-dynamic flight segments. Without the yaw AM measurement (i.e., for the conventional IVM-only filter), z-gyro drift and heading error can only be estimated during maneuvers. Thus heading error increases without bound (as the integral of z-gyro drift) during low-dynamic segments.

The benefits afforded by the MICA filter are illustrated in Figure 2.2-1 where the heading and z-gyro drift one-sigma errors projected by TRANSIM are shown for a typical s-turn alignment trajectory. (In this figure, the MICA filter results are designated by the curves labeled IVM/AM. Also, the true gyro drift errors were initialized at 50 deg/hr rather than 100 deg/hr for this run.) During the two heading changes, executed roughly 100 sec and 220 sec into the alignment, IMU heading and z-gyro errors converge for the two filters. However, during the straight-and-level alignment segments, the errors increase for the IVM filter but remain nearly constant for the MICA filter. The simulation indicates that the reduced alignment errors associated with the MICA filter translate into a 50% reduction in CEP over a 60-sec post-alignment, glide-bomb trajectory. This reduction is illustrated in Figure 2.2-2.

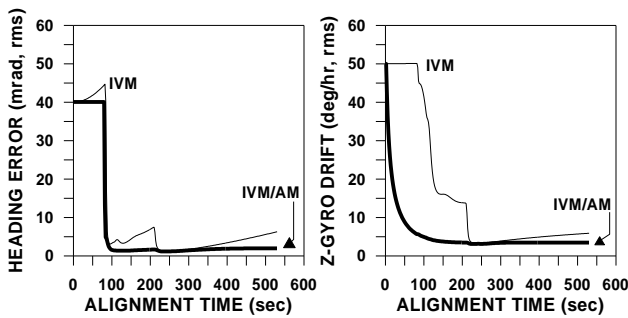


Figure 2.2-1 Simulation Results for a S-Turn Alignment

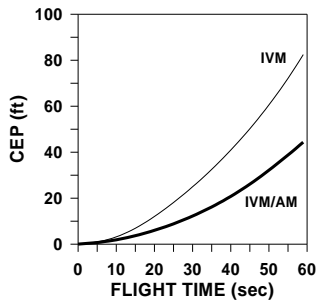


Figure 2.2-2 Simulated CEP Following S-Turn Alignment

3. LABORATORY TESTS

3.1 TEST PREPARATION

The primary objectives of laboratory tests were to: (1) verify MICA equipment performance and system integration, and (2) assess the performance of the MICA filter when operating in a benign environment. Following integration tests, a laboratory test configuration was designed and fabricated. This configuration involved mounting both the MEMS IMU and IFMU to a rigid aluminum plate, which was designed to provide and maintain an accurate alignment of the IMU and IFMU case frames. The aluminum plate was then mounted to a 17" square aluminum slab, which was

designed to align the plate with the H-423 INS mount (see Figure 3.1-1).

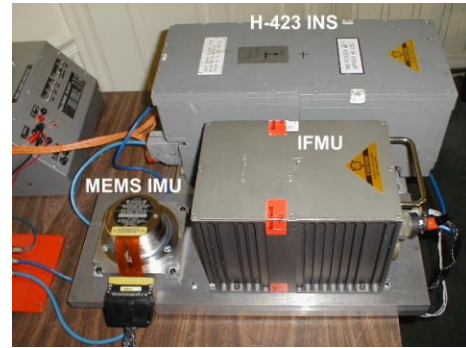


Figure 3.1-1 MICA Laboratory Test Configuration

The residual misalignment angles between the inertial equipment on the slab were accurately measured using both a least-squares algorithm and System Dynamics' rapid transfer alignment (RAP) algorithm. The least-squares algorithm processed accelerometer data collected from the IFMU and IMU at three different roll orientations to estimate the misalignments between the IFMU and IMU body frames. The RAP algorithm processed inertial data from the INS and IFMU to estimate the misalignments between the INS and IFMU body frames.³⁻⁴ Ultimately, the INS-to-IMU slab misalignments were computed to be -0.7 mrad in roll, 1 mrad in pitch, and 6 mrad in yaw (to within an accuracy of roughly 0.5 mrad). These values were used as the "reference" misalignments during laboratory and van tests.

3.2 TEST RESULTS

A total of 24 valid laboratory tests were conducted to assess filter performance. These tests involved either 300-sec stationary scenarios, where the slab remained motionless during alignment, or 300-sec dynamic scenarios, where the slab was rotated during alignment to impart roll and/or yaw motions. For all tests, alignment was typically terminated after roughly 220 sec and the IMU was then allowed to navigate in the post-alignment mode for the remaining 80 sec (in order to quantify post-alignment IMU navigation error growth).

At the beginning of each test, the IMU's attitude angles were automatically initialized by the test software as the sum of the INS-indicated attitude angles and three user-defined misalignment angles (entered via a user-interface menu). For all tests, the misalignment angles were defined in the menus to be 10 mrad in roll and pitch and 0 mrad in yaw, rather than the actual -0.7 mrad, 1 mrad, 6 mrad reference misalignment values described above. These definitions established the IMU's initial attitude errors (relative to the INS) to be 10.7 mrad in roll, 9 mrad in pitch, and -6 mrad in yaw. During alignment, each filter attempted to estimate

and correct these attitude errors (as well as other modeled errors such as IMU gyro drifts).

Alignment Accuracy: Filter alignment accuracy was assessed by first computing the differences between the IMU and INS indicated attitude angles (i.e., the roll, pitch, and yaw differences) at the end of alignment to determine the residual misalignments, and then subtracting the known reference misalignments from these values. The resulting values defined the filter's attitude estimation errors. In a perfect system, the INS/IMU attitude angle differences would equal the known misalignments, yielding zero filter attitude estimation errors. (Zero (or small) filter attitude estimation errors indicate that the filter correctly estimates the IMU's attitude relative to the INS.)

The IMU's roll and pitch attitude errors remaining at the end of alignment are illustrated in Figure 3.2-1 for the MICA and IVM-only filters. The results indicate that the MICA and IVM filters yield nearly identical results in roll and pitch (in fact, the histograms are identical), and accurately estimate roll and pitch errors (as evidenced by the small means and standard deviations).

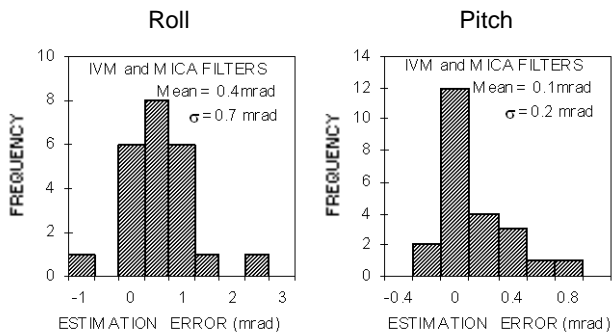


Figure 3.2-1 Lab IMU Roll and Pitch Alignment Errors

It is important to note that in a laboratory environment, IMU yaw (heading) error is not observable and thus cannot be accurately estimated by either the MICA or IVM filters. Consequently, it is reasonable to assume that the yaw estimation errors at the end of alignment for the two filters should remain close to the initial -6 mrad misalignment error. As shown in Figure 3.2-2, this was indeed the case for the MICA filter but not for the IVM filter. The MICA filter exploits yaw AM measurements to maintain IMU yaw error near its initial value. However, the IVM filter has no mechanism to prevent yaw error from increasing as the integral of z-gyro drift.

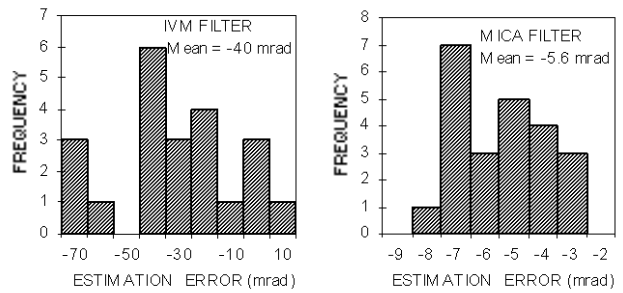


Figure 3.2-2 Lab IMU Yaw Alignment Errors

Gyro Calibration Accuracy: The filters' gyro drift estimation accuracy was determined by first determining the IMU's true gyro drift and then subtracting it from the filters' estimate of the drift. The true gyro drift was computed by subtracting the true angular rate from the IMU-indicated angular rate. For stationary laboratory tests, the true angular rate was simply the known earth-rate vector expressed in IMU body coordinates. The IMU-indicated angular rate was formed by summing the 100 Hz $\Delta\theta$ s over the entire alignment time and then dividing by the alignment time.

Figure 3.2-3 illustrates the $\Delta\theta$ gyro data collected from the MEMS IMU (left side) and the more accurate IFMU (right side) for a typical stationary laboratory test (designated as Test 43). The plots depict one-second averages of $\Delta\theta$ data with the earth rate components removed. As expected, the MEMS gyros exhibit much larger drift rates (as noted by their mean values) than do the IFMU's GG1308 RLGs. Also, the MEMS gyros exhibit a noticeable in-run stability.

Figure 3.2-4 illustrates the MEMS gyro drift rates estimated by both the MICA and the IVM filters for Test 43. The figure indicates that both filters quickly and accurately estimate the x- and y-gyro drifts, as evidenced by the convergence of the estimates to the true drift values shown in Figure 3.2-3. However, as expected, due to the absence of any maneuver, only the MICA filter affords a continuous estimation of z-gyro drift, thereby demonstrating one of the primary benefits of the MICA algorithm. In contrast, the IVM filter's z-gyro estimate remains close to zero, resulting in a -40 deg/hr gyro estimation error. This gyro error is in fact the source of the heading error growth included in Figure 3.2.2 for the IVM filter.

Figure 3.2-5 summarizes the MICA and IVM z-gyro drift estimation errors for laboratory tests. With the exception of two outliers, the figure indicates that the MICA filter estimates IMU z-gyro drift rate to within an accuracy of 5 deg/hr. Conversely, the IVM filter was unable to accurately estimate z-gyro drift due to the absence of a significant maneuver. Although not shown, the results also indicated that both filters estimated the x- and y-gyro drift rates to within an accuracy of 5 deg/hr (via the common IVM measurements).

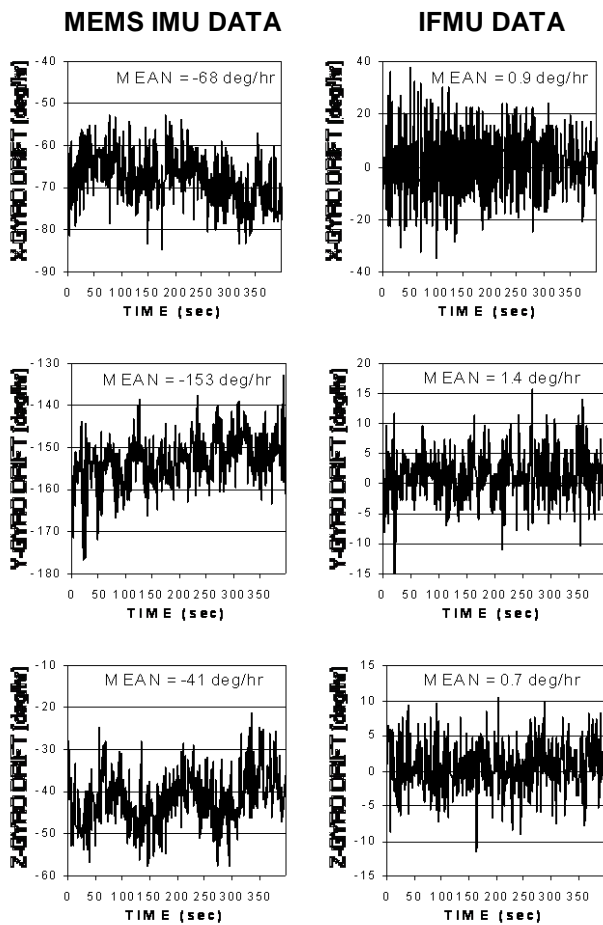


Figure 3.2-3 Gyro Drift Data for Laboratory Test 43

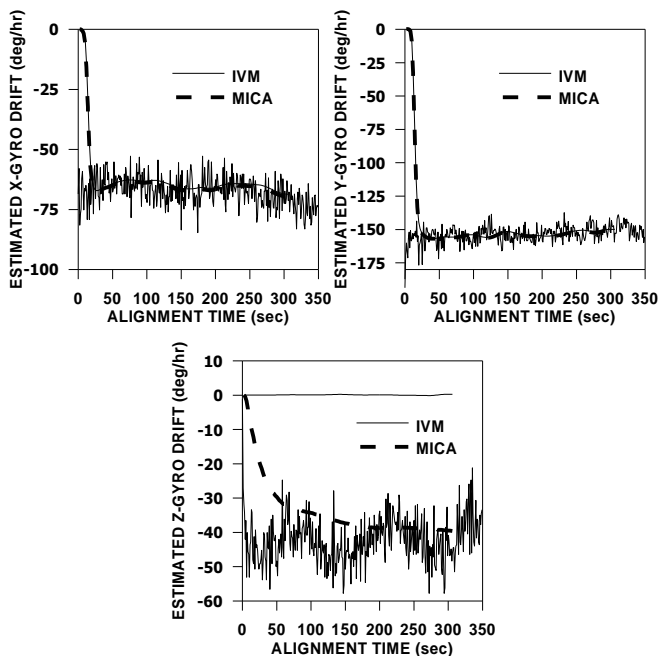


Figure 3.2-4 Gyro Drift Estimates for Laboratory Test 43

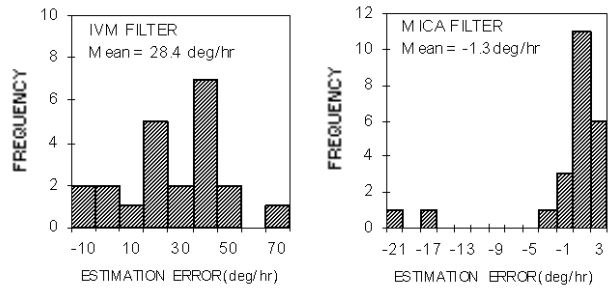


Figure 3.2-5 Summary of Z-Gyro Drift Estimation Errors

4. VAN TESTS

4.1 TEST PREPARATION

Van tests were conducted with the MICA equipment installed in the AFRL/MNGN Mobile Test Vehicle (MTV) at Eglin AFB. As for lab tests, the inertial equipment remained bolted to the aluminum slab for all van tests. Figure 4.1-1 shows the MICA equipment suite which was placed on a level surface located directly behind the driver's seat. The equipment was powered by DC power supplies connected to the van's AC power bus. Tests were monitored using one of the van's computer workstations.

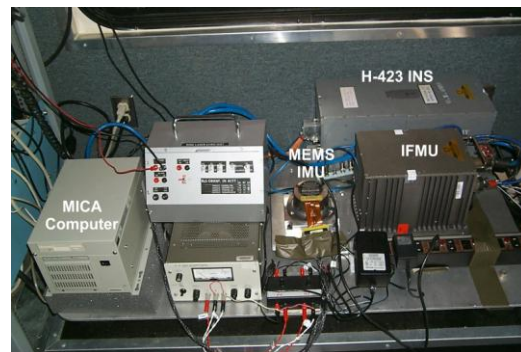


Figure 4.1-1 MICA Equipment in the MTV

A total of 27 van tests were conducted to assess filter performance in a moderate-dynamic environment. These tests included 15 tests conducted while the van traveled over winding access roads and 12 tests conducted while the van traveled over a prescribed trajectory at abandoned Runway C3. The majority of van tests involved an alignment segment exceeding 300-sec followed by a 60-100 sec post-alignment segment.

Although test data collected over Eglin's access roads yielded valuable results, the van's trajectory could not be readily controlled due to local traffic constraints. More flexibility was afforded on the abandoned runway, however, where a prescribed van trajectory could be performed. Most runway tests were specified to include a straight constant-velocity segment (e.g., 30 mph) followed by a 90-deg turn and a deceleration to rest. The van remained at rest for

several hundred seconds and then turned 90-deg (to the original heading) and continued straight until the test was terminated. Transfer alignment was initiated during the initial constant velocity segment and terminated at the completion of the rest segment. The lengthy rest segment was included to evaluate alignment persistence; i.e., the ability of the MICA filter to maintain alignment accuracy following the alignment maneuvers (in this case, following the first 90-deg turn).

4.2 TEST RESULTS

Since test profiles conducted on the runway (vice access roads) are more compatible with those planned for flight tests, the runway test results will be emphasized herein. These results are summarized in the following paragraphs.

Alignment Accuracy: As for laboratory tests, filter alignment accuracy for van tests was assessed by first computing the differences between the IMU and INS indicated attitude angles (i.e., the roll, pitch, and yaw differences) at the end of alignment to determine the residual misalignments, and then subtracting the known reference misalignments from these values. The resulting values defined the filter's attitude estimation errors.

The IMU's roll and pitch attitude errors remaining at the end of alignment for the runway tests were similar to those presented previously for laboratory tests. Specifically, the roll and pitch errors quickly converged to relatively small values (with means and standard deviations less than 1.2 mrad), and the roll and pitch error behaviors were nearly identical for the two filters. However, as expected, the yaw errors were much larger and dramatically different for the two filters.

Figure 4.2-1 summarizes the IMU yaw errors at the end of alignment for the 12 runway tests. Note that the IVM filter incurs large yaw errors, while the MICA filter maintains the yaw errors near their initial values. This behavior is due to the fact that the MICA filter is capable of accurately calibrating IMU z-gyro drift in the low-dynamic van-test environment while the IVM filter is not. Thus, for the IVM filter, the large (uncorrected) z-gyro drift propagates directly into a large IMU yaw error during alignment. Although yaw error growth is also exhibited by the MICA filter (roughly 3 mrad, from the -6 mrad reference to the -3.2 mean value shown in Figure 4.2-1), the growth rate is much smaller because the MICA filter accurately calibrates the z-gyro during alignment (see following paragraphs).

Gyro Calibration Accuracy: As for laboratory tests, the filters' gyro drift estimation accuracy for van tests was assessed by first determining the IMU's true gyro drift and then subtracting it from the filters' estimate of the drift. The true gyro drift was computed by subtracting the true angular rate from the IMU-indicated angular rate. For the lengthy

rest segment during alignment, the true angular rate was simply the known earth-rate vector expressed in IMU body coordinates. The IMU-indicated angular rate was formed by summing the 100 Hz $\Delta\theta$ s over the rest segment and then dividing by the segment time.

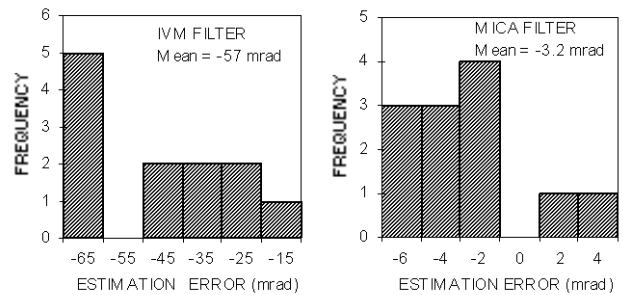


Figure 4.2-1 Van IMU Yaw Alignment Errors

Figure 4.2-2 illustrates the true gyro drift rates exhibited by the IMU for a typical runway test (designated as Test 33) during the rest segment (from the 49-sec point until the 320 sec point). Specifically, the plots depict one-second averages of IMU $\Delta\theta$ data with the earth rate components removed. As expected based on laboratory test results, the plots reveal relatively large mean values (i.e., large fixed drift rates) and significant in-run stability errors (as evidenced by the imaginary trend line).

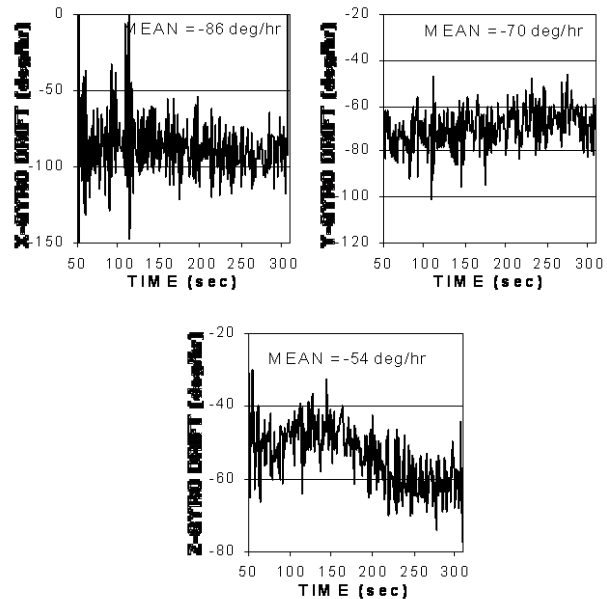


Figure 4.2-2 IMU Gyro Drift Rates for Van Test 33

Figure 4.2-3 illustrates the gyro drift rates estimated by both the MICA and the IVM filters for Van Test 33. The figure indicates that both filters quickly and accurately estimate the x- and y-gyro drifts, as evidenced by the convergence of the estimates to the true drift values shown in Figure 4.2-2. However, as for laboratory tests, only the MICA filter accurately estimates the z-gyro drift. The IVM filter z-gyro

estimate remains close to zero, resulting in a -54 deg/hr estimation error.

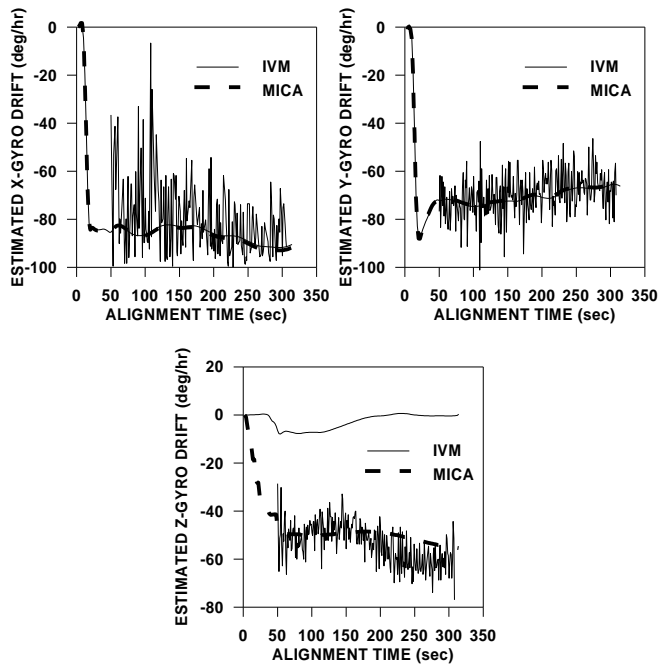


Figure 4.2-3 Gyro Drift Estimates for Van Test 33

The corresponding IMU yaw (heading) attitude errors incurred during alignment for Test 33 are presented in Figure 4.2-4. As described above, since the IVM filter is not capable of estimating z-gyro drift during the low-dynamic van trajectory, IMU yaw error increases unbounded as the integral of the large z-gyro drift. Conversely, the MICA filter exploits its yaw AM measurements to both bound IMU yaw error growth and accurately estimate z-gyro drift.

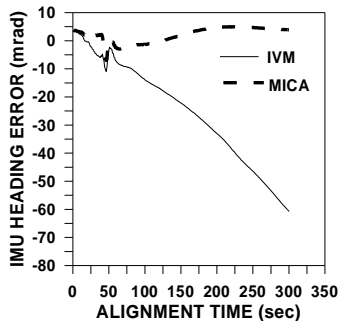


Figure 4.2-4 IMU Yaw (Heading) Error for Van Test 33

Figure 4.2-5 summarizes the IMU z-gyro drift rates remaining at the end of alignment for the 12 runway tests. The results demonstrate that the MICA filter accurately calibrates IMU z-gyro drift during alignment and maintains the calibration over the lengthy rest segment. Conversely, the IVM filter is unable to calibrate z-gyro drift and thus exhibits significantly larger z-gyro drift rates. It should be noted that the inability of the IVM filter to calibrate the z gyro is due primarily to insufficient dynamics incurred

during the van trajectory. The dynamics incurred during flight are sufficient for the IVM filter to observe and calibrate the z gyro, but only during heading changes.

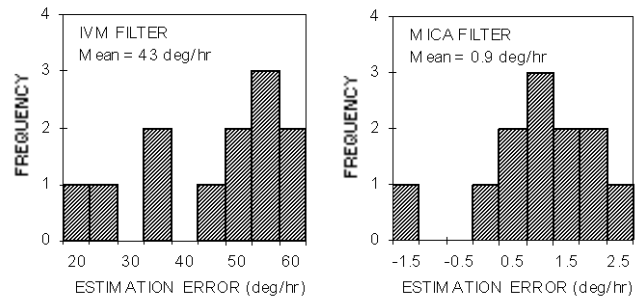


Figure 4.2-5 Z-Gyro Drift Estimation Errors (Van Tests)

5. FLIGHT TESTS

5.1 TEST PREPARATION

Following van tests, the MICA equipment was removed from the aluminum slab and installed in a Block 30 F-16C test aircraft. Specifically, the IMU and IFMU (which remained bolted to the rigid plate) were installed in the GI pod along with the MICA computer. The pod was then secured to weapon station #3 on the F-16. The H-423 INS was installed behind the cockpit in the ammo drum while the Termiflex controller was installed in the cockpit. Figure 5.1-1 shows the equipment in the GI pod. Ground mount tests were conducted to verify equipment installation, and the lever-arm displacement vector from the INS to the IMU was measured.



Figure 5.1-1 MICA Equipment in GI Pod

The MICA flight test plan specified four 1.5-hour sorties at Eglin AFB. During each sortie, a series of 500-sec captive-carry tests were conducted, thereby allowing between eight to ten tests per sortie. Each test included a typical 400-sec transfer alignment trajectory followed by a 100-sec post-alignment trajectory. One of two alignment trajectories was flown for each test. The alignment trajectories included an initial 100-sec segment during which time the prescribed alignment maneuvers were conducted (i.e., either one or two 30-deg heading changes), followed by a 300-sec straight-

and-level (SAL) segment. The SAL segment was included to evaluate alignment persistence; i.e., the ability of the filter to maintain alignment accuracy during the non-maneuvering segment prior to weapon release. One of three post-alignment trajectories was also flown for each test. These trajectories included an initial 50 kt deceleration period followed by a period of prescribed dynamics. The MICA flight test trajectories are described in Table 5.1-1.

Table 5.1-1 Planned MICA Flight Test Trajectories

<p>Alignment Trajectories: (400-sec duration, 300 kts, 5000 ft AGL):</p> <ol style="list-style-type: none"> One-Turn: After 30-sec of SAL flight, execute one 30-deg turn, then continue SAL for roughly 350 sec (until the 400-sec point) S-Turn: After 30-sec of SAL flight, execute two 30-deg turns, then continue SAL for roughly 350 sec (until the 400-sec point) High-Altitude S-Turn: S-turn trajectory at 20,000 ft AGL
<p>Post-Alignment Trajectories (100-sec duration):</p> <ol style="list-style-type: none"> Smoother: Decelerate 50 kts and continue SAL until 60 sec, then execute 90-deg turn (follows either one-turn or s-turn alignment) Weapon: Decelerate 50 kts then execute gradual 20-deg skidded turn until end (follows either one-turn or s-turn alignment) High-Altitude Weapon: Following high-altitude s-turn alignment, decelerate 50 kts and descend to 5000 ft while executing a gradual 20-deg skidded turn

The weapon post-alignment trajectories shown in Table 5.1-1 were specified to represent the dynamics of an unpowered weapon while the smoother trajectory was specified to facilitate post-test analyses. For example, while the first 60-sec of the smoother trajectory represents the dynamics of a benign weapon trajectory, the subsequent 90-deg turn excites IMU alignment errors which can be estimated by a post-test Kalman smoother.

For each test, the IMU was transfer aligned with both the MICA filter and the conventional IVM filter using two separate software channels to maintain two independent alignment and navigation solutions (i.e., one associated with the MICA filter and the other associated with the IVM filter). During post-test analyses, the results were contrasted to quantify the potential accuracy improvements associated with the MICA filter.

5.2 TEST RESULTS

To date, two of the four sorties have been completed; however, the data analyses has only been partially completed. During these sorties, a total of nineteen valid 500-sec tests were conducted. These tests involved a combination of the one-turn and s-turn alignment trajectories along with the smoother and weapon post-alignment trajectories (refer to Table 5.1-1). The initial results indicate that the MICA filter is capable of improving IMU alignment accuracy (particularly IMU heading accuracy and z-gyro drift calibration) and ultimately post-alignment IMU navigation accuracy.

Figure 5.2-1 presents the plan view of a typical alignment test conducted during the first sortie (designated as Test 1_4). For this test, the aircraft executed an s-turn alignment trajectory (at an initial heading of 150 deg) and the smoother post-alignment trajectory.

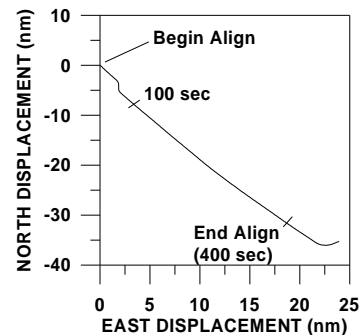


Figure 5.2-1 Plan View for Flight Test 1_4

Figure 5.2-2 illustrates angular rate data collected from the IMU (left) and the H-423 INS (right) during 300 seconds of the SAL segment. These plots depict instantaneous 1-sec samples of angular rate from the two inertial devices. The greater variability exhibited by the IMU data is primarily due to two factors: (1) true angular rate differences between the fuselage-mounted INS and the pod-mounted IMU (i.e., relative motion), and (2) the noisy behavior of the MEMS gyros relative to the INS's GG1342 RLGs.

The alignment accuracy of the MICA filter will be assessed using three techniques. The first technique employs a Kalman smoother to process IMU navigation errors incurred over the smoother post-alignment trajectory. The smoother employs stochastic models of inertial error behavior to "back-out" IMU alignment/calibration errors based on how these errors propagate into position/velocity errors following the completion of alignment⁵. The second technique compares IMU position errors following alignment with two-sigma position errors projected using a model-based covariance simulation. The simulation is initialized assuming that an accurate alignment has indeed occurred. Thus, an accurate IMU alignment is inferred if the actual post-alignment position error traces fall within the two-sigma error bounds. The third technique computes the differences between the INS and IMU-indicated attitude angles computed during alignment. Recall that during alignment, filter estimates are used to correct IMU sensor outputs and navigation quantities computed in the IMU strapdown equations. Thus, an accurate alignment occurs if the attitude differences converge to the actual misalignment angles between the INS and IMU. For laboratory and van tests, the actual misalignment angles are precisely known, as a result of the slab-mounted equipment configuration. However, for flight tests, the actual misalignment angles are not precisely known. Nevertheless, the alignment attitude differences for the MICA and IVM filters can be contrasted to examine the behavior of the two filters.

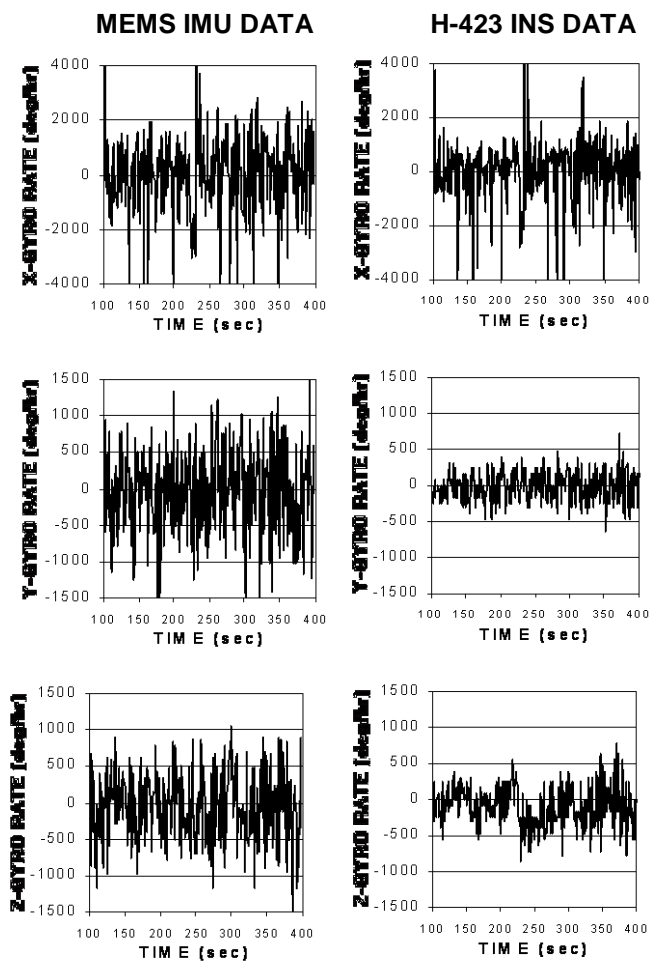


Figure 5.2-2 IMU and INS Angular Rates (Test 1_4)

Alignment results for Test 1_4 are illustrated in Figure 5.2-3. In the figure, the IMU minus INS attitude differences are shown for both the MICA and IVM filters. The plots indicate that: (1) the roll and pitch (level-axes) differences converge to (and are maintained at) the same values for the two filters, (2) the yaw differences converge to the same values for the two filters following the completion of the s-turn (at roughly 80 sec), and (3) the yaw differences diverge for the two filters during the subsequent 320-sec SAL segment. These results suggest that, as predicted by simulation, the MICA filter suppresses the IMU's heading error growth during alignment while the IVM filter allows IMU heading error to grow as the integral of uncorrected z-gyro drift. (Note that the rather large attitude differences which occur during the s-turn are due primarily to uncompensated time-sync errors between the INS and IMU.)

The yaw-difference growth associated with the IVM filter in Figure 5.2-3 corresponds to a filter mis-estimation of the z-gyro drift by roughly 13 deg/hr. Figure 5.2-4, which presents z-gyro drift estimates for this test, indicates that the MICA and IVM filter estimates indeed differ by nearly 13

deg/hr. (The thin dashed line in Figure 5.2-4 represents the drift rate reference value. This reference was computed as the difference in the mean values between the IMU and INS z-gyro rates shown in Figure 5.2-2.)

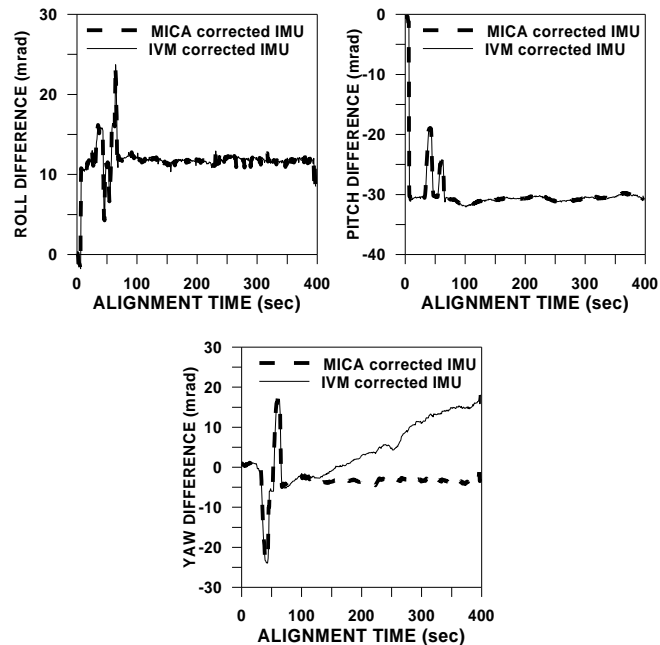


Figure 5.2-3 Alignment Attitude Differences (Test 1_4)

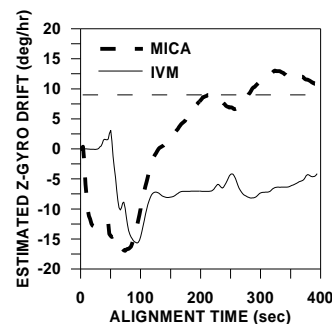


Figure 5.2-4 Estimates of IMU Z-Gyro Drift (Test 1_4)

The IMU's post-alignment horizontal position errors for Test 1_4 are illustrated in Figure 5.2-5 over the first 60 seconds of the post-alignment trajectory (prior to the 90-deg turn). The horizontal position errors are computed by calculating the IMU minus INS north and east position differences and then rss'ing the two components. Note that at the end of alignment (t = 400 sec), IMU position is re-initialized with INS position compensated for the known lever-arm displacement. Thus, the slowly-varying INS position errors (and also INS velocity and attitude errors) cancel out in the difference. Consequently, any growth in the horizontal position difference between the INS and the IMU can be attributed to IMU alignment/calibration errors. Figure 5.2-5 illustrates that for this test, the MICA alignment achieves a 33% (13 m) reduction in horizontal position error. This

reduction can be traced to the reduced heading error associated with the MICA filter. (For this trajectory, IMU heading error is excited during the initial deceleration period.) Two-sigma error bounds projected by the MICA covariance simulation will ultimately be computed and superimposed on the plot, and the Kalman smoother will be run to further assess filter performance. Nonetheless, it is important to note that the MICA horizontal position error for this test is consistent with that expected for a 5-10 deg/hr IMU.

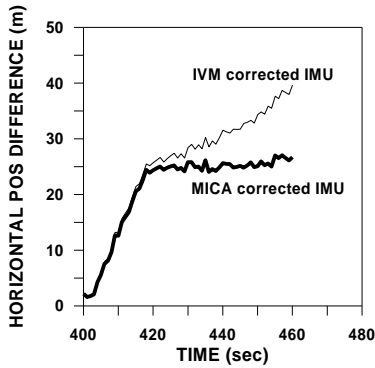


Figure 5.2-5 Post-Alignment Position Difference (Test 1_4)

The attitude differences for a one-turn alignment test conducted during the second sortie are shown in Figure 5.2-6 (designated as Test 2_3). Much like Figure 5.2-3, the plots indicate that the two filters perform equally well for the roll and pitch axes, but the yaw differences diverge for the two filters during the 300-sec SAL segment. Again, this indicates that the MICA filter suppresses the IMU's heading error growth during alignment while the IVM filter allows IMU heading error to grow as the integral of uncorrected z-gyro drift.

The IMU's post-alignment horizontal position errors for this test are illustrated in Figure 5.2-7 over the 100-sec “weapon” trajectory (see Table 5.1-1). Here, the MICA alignment achieves roughly a 25% (30 m) reduction in horizontal position error after 100 seconds of flight. Again, this reduction is a direct consequence of the reduced heading error associated with the MICA filter.

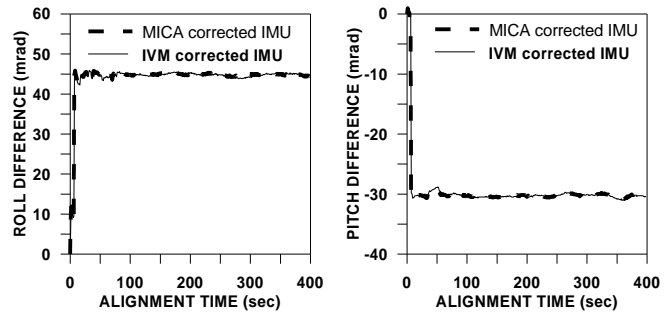


Figure 5.2-6 Alignment Attitude Differences (Test 2_3)

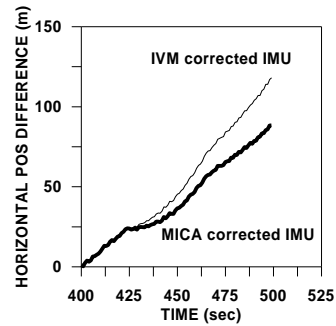
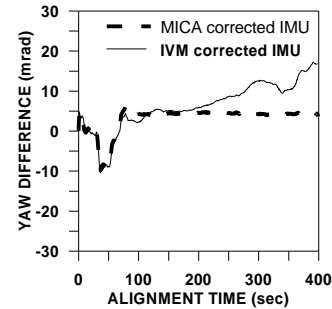


Figure 5.2-7 Post-Alignment Position Difference (Test 2_3)

6.

CONCLUSIONS

Simulation and test results were presented which indicate that modifying the conventional integrated-velocity-match (IVM) filter to include yaw attitude-match (AM) measurements significantly improves the alignment and navigation accuracy of a low-grade MEMS IMU. Specifically, the yaw AM measurements were shown to provide improvements in z (yaw) gyro calibration along with a significant reduction in heading error growth following the completion of the alignment maneuvers. Although flight tests are on-going, initial results have indicated that the MICA filter significantly improves IMU alignment and calibration, resulting in an unaided navigation performance similar to that expected for a 5-10 deg/hr system. If these results are borne out by the remaining flight tests, then a 100

deg/hr MEMS IMU when aligned with the MICA (or similar) filter, may indeed provide a cost-effective alternative to optical-gyro IMUs.

ACKNOWLEDGEMENTS

This work was supported by the Air Force Research Laboratory Munitions Directorate (AFRL/MN) at Eglin AFB under the SBIR Phase II program (Contract No. F08630-99-C-0025).

REFERENCES

- [1] Graham, W.R. and Shortelle, K.J., "Munition Flight Mechanics Research", Report No. AFRL-MN-EG-TR-1998-7022, Contract No. F08630-98-C-0069, February 1999.
- [2] Graham, W.R. and Shortelle, K.J., "Transfer Alignment of MEMS IMUs for Tactical Applications", unpublished technical paper based on Report No. AFRL-MN-EG-TR-1998-7022, February 1999.
- [3] Graham, W.R. and Shortelle, K.J., "Rapid Alignment Prototype (RAP) Flight Test Demonstration", Institute of Navigation National Technical Meeting, Long Beach, CA, January 1998.
- [4] Shortelle, K.J. and Graham, W.R., "F-16 Flight Tests Results of a Rapid Transfer Alignment Procedure", IEEE Position, Location, and Navigation Symposium, Palm Springs, CA, April 1998.
- [5] Graham, W.R. and Shortelle, K.J., "MEMS IMU Calibration and Alignment (MICA)", System Dynamics International, Inc., Final Report, In Progress.